WEIGHT FUNCTION METHOD FOR DETERMINATION OF CRITICAL PLANE POSITION UNDER MULTIAXIAL LOADING

R. Brighenti*, A. Carpinteri*, E. Macha† and A. Spagnoli*

The expected fracture plane can be determined according to the critical plane approach and the fatigue life of a body under multiaxial loading can be calculated. A critical plane method recently proposed by the authors consists in averaging the instantaneous values of the three Euler angles, which describe the principal stress directions, through some suitable weight functions to take into account the main factors influencing fatigue fracture behaviour. Such a method is applied to a number of experimental biaxial proportional and non-proportional sinusoidal stress states.

INTRODUCTION

Several criteria exist to predict the fatigue life of a body under multiaxial stress conditions. One group of fatigue criteria is based on the critical plane approach (You and Lee (1), Papadopoulos et al (2)), according to which the critical or expected fracture plane is determined and the fatigue life can be calculated. As is shown by many test results obtained under multiaxial cyclic loading, the fatigue fracture plane position chiefly depends on the directions of the maximum principal stress or strain and the maximum shear stress or strain (Macha (3-4)). However, in many cases we observe changes of the principal axes positions and this fact cannot be neglected.

Factors influencing the position of the critical plane can be accounted for through an averaging procedure. The weight function method consists in averaging the instantaneous values of the parameters which determine the position of the principal stress or strain axes, by employing some suitable weight functions (Macha (4)) which are assumed to take into account the main factors influencing fatigue fracture behaviour.

In this work, the weight function method presented in Carpinteri et al (5) for predicting the expected fatigue fracture plane position under multiaxial random loading is assessed through experimental data obtained under biaxial proportional and non-proportional sinusoidal stress states.

* Department of Civil Engineering, University of Parma, Italy.
† Department of Mechanics and Machine Design, Technical University of Opole, Poland.

EXPECTED CRITICAL PLANE POSITION

The matrix A of the principal direction cosines l_n, m_n, n_n, $n = 1,2,3$ (the principal stresses are arranged so as $\sigma_1 \geq \sigma_2 \geq \sigma_3$) consists of nine elements, but only three of them are independent because of six orthonormality conditions. Alternatively, the orthogonal coordinate system P123 of the principal directions can be described through the Euler angles ϕ, θ, ψ (Fig. 1). This allows us to avoid the controversial problem of selecting 3 independent parameters (from the matrix A) to be used in the ensuing averaging procedure (Ref. (5)).

The calculation of the Euler angles at time instant t_k from the matrix $A(t_k)$ consists of two stages. In the first stage (1st reduction), the Euler angle ranges $0 \leq \phi(t_k), \psi(t_k) < 2\pi$ and $0 \leq \theta(t_k) < \pi$ (Korn and Korn (6)) are reduced to the new range $-\pi/2 \leq \phi(t_k), \theta(t_k), \psi(t_k) \leq \pi/2$ by multiplying particular columns of the matrix $A(t_k)$ by ± 1.

In the second stage (2nd reduction), the signs of the above results are changed in order to average the values of the Euler angles in a correct way with respect to their physical meaning. Consider the vector $(C-P)$ which describes the position of the X-axis (Fig. 2). Such a vector moves because of the three sequentially combined rotations $\phi(t_k), \theta(t_k), \psi(t_k)$, and reaches the final position representative of the 1-axis. Since the Euler angles range from $-\pi/2$ to $\pi/2$ after the 1st reduction, eight possible final positions can be determined according to the different combinations of their signs (Fig. 2). Four sign combinations represent the possible positions E_1, E_2, E_3 and E_4 of the 1-axis on an external cone, while the other four combinations represent the positions I_1, I_2 I_3 and I_4 on an internal cone. Thus, the first four combinations describe a unique solid angle between the X-axis and the 1-axis, while the second four combinations determine another value of such a solid angle. For this reason, the signs of $\phi(t_k), \theta(t_k), \psi(t_k)$ deduced through the 1st reduction are changed to correctly average the Euler angles. For example, we can assume the sign combination (+,+,+) for the cases E_1, E_2, E_3 and E_4 relative to the external cone, and the combination (+,+,-) for the I_1, I_2 I_3 and I_4 relative to the internal cone. In this way (2nd reduction) the ranges of the Euler angles are reduced as follows: $0 \leq \phi(t_k), \theta(t_k) \leq \pi/2$ and $-\pi/2 \leq \psi(t_k) \leq \pi/2$.

Since the expected fatigue fracture plane position is here assumed to depend on the mean directions of the principal stress axes $\hat{1}$, $\hat{2}$ and $\hat{3}$, the weighted averaging of the Euler angles is carried out by employing the following weight function, $W(t_k)$:

$$W(t_k)=\begin{cases} 0 & \text{if } \sigma_1(t_k)<c\,\sigma_{af} \\ & 0<c\le 1 \\ \left[\sigma_1(t_k)/(c\,\sigma_{af})\right]^{m_\sigma} & \text{if } \sigma_1(t_k)\ge c\,\sigma_{af} \end{cases} \qquad (1)$$

that includes into the averaging process those positions of the principal axes for which the maximum principal stress σ_1 is greater than or equal to the product of the constant coefficient c, with $0 < c \le 1$, and the fatigue limit stress, σ_{af}, deduced from the S-N curve plotted for loading ratio equal to -1. The weight of such positions exponentially depends on the coefficient $m_\sigma = -1/m$, where m is the slope of the S-N curve being considered. In Fig. 3, the weight function $W(t_k)$ for $c < 1$ is plotted for a generic time history of the maximum principal stress, together with the function $\phi * W$ to be averaged to determine the expected Euler angle $\hat{\phi}$.

EXPERIMENTAL ASSESSMENT

The method described in the previous section is applied to analyse the results obtained from synchronous sinusoidal fatigue tests on thin-walled cylinders under (σ_x, σ_y) stress state, where the X-axis coincides with the longitudinal axis of the specimens, (Rotvel (7)), and on round bars under (σ_x, τ_{xy}) stress state (Nishihara and Kawamoto (8)).

Rotvel's specimens were made of carbon steel with 0.35% C content, yield stress σ_0 = 255.0 MPa, Young modulus E = 210 GPa, Poisson ratio ν = 0.29, σ_{af} = 215.8 MPa, m_σ = 14.5. Non-zero mean stresses, σ_{xm} and σ_{ym}, and phase angles, δ, equal to 0 or π, were applied (Table 1). Nishihara's specimens were made of Swedish hard steel with 0.51% C content, σ_0 = 392.4 MPa, E = 200 GPa, ν = 0.30, σ_{af} = 313.9 MPa, m_σ = 8.7. Zero mean stresses, σ_{xm} and τ_{xym}, and δ = 0 or $\pi/6$ were applied (Table 2). Various amplitudes (σ_{xa}, σ_{ya} and σ_{xa}, τ_{xya}) of the applied stresses were considered in both test series.

The fatigue fracture plane position can be defined through the angle η between the normal to the fracture plane and the specimen axis. By assuming that the normal to the expected fatigue fracture plane agrees with the weighted average direction of the maximum principal stress, the theoretical value η_{cal} is calculated. The comparison of Rotvel's and Nishihara's experimental results (η_{exp}) with our theoretical predictions is presented in Tables 1 and 2, respectively (the expected critical plane is calculated by assuming c = 0.5). Figures 4 and 5 show a fragment of the time history in the period, T, for the applied and principal stresses and for the reduced Euler angles used in the averaging procedure, for Rotvel's test No. 6 and Nishihara's test No. 3, respectively.

CONCLUSIONS

The principal stress directions change at each time instant, even under sinusoidal loading. The theoretical procedure to calculate the three Euler angles of the principal stress directions from the matrix of the principal direction cosines (Carpinteri et al (5)) is used here to assess biaxial sinusoidal fatigue test data. The agreement between theoretical and experimental results is quite satisfactory.

REFERENCES

(1) You, B.-R. and Lee, S.-B., Int J Fatigue, Vol. 18, 1996, pp. 235-244.

(2) Papadopoulos, I.V., Davoli, P., Gorla, C., Filippini, M. and Bernasconi, A., Int J Fatigue, Vol. 19, 1997, pp. 219-235.

(3) Macha, E., Fortschr.-Ber.VDI, Vol. 18, 1988, 102.

(4) Macha, E., Mat.-wiss.u.Werkstofftech, Vol. 20, 1989, pp. 132-136 and 153-163.

(5) Carpinteri, A., Macha, E., Brighenti, R., Brys, R., Spagnoli, A., Proceeding 5th International Conference on Biaxial/Multiaxial Fatigue and Fracture (5 ICBMFF), Edited by E. Macha and Z. Mroz, Vol. 1, pp. 541-555, Cracow, Poland, 1997.

(6) Korn, G.A. and Korn, T.M., "Mathematical Handbook", McGraw-Hill Book Company, New York, 1968.

(7) Rotvel, F., Int J Mech Science, Vol. 12, No. 7, 1970, pp. 597-613.

(8) Nishihara, T. and Kawamoto, M., Memories of the College of Engineering, Kyoto Imperial University, Vol. 11, No. 4, 1945, pp. 85-112.

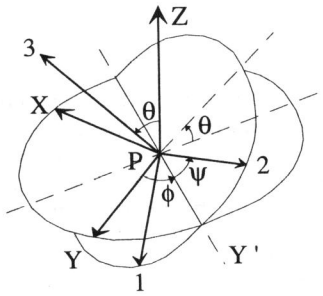

Fig. 1. Principal stress directions 123 described through the Euler angles ϕ, θ, ψ.

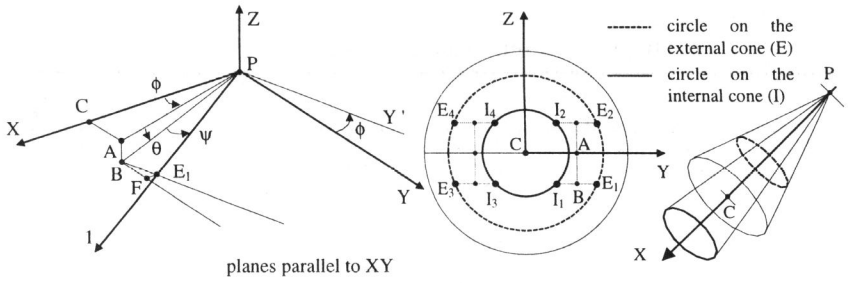

Fig. 2. Sequentially combined rotations ϕ,θ,ψ from the X-axis to the 1-axis and their eight different combinations.

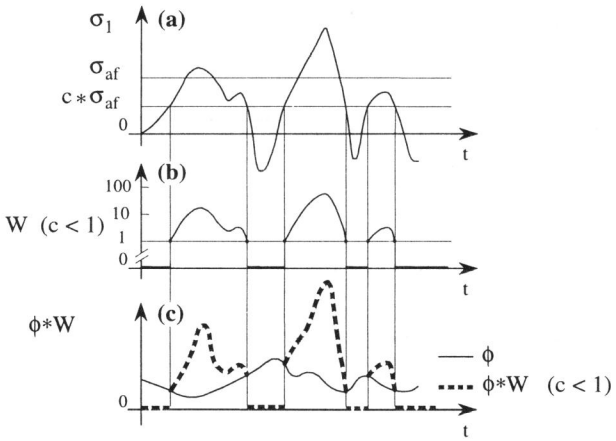

Fig. 3. Modifications of the time history of angle $\phi(t)$ by means of weight function $W(t)$.

TABLE 1 - Comparison of experimental and calculated fatigue fracture plane position for Rotvel's tests (7).

	σ_{xa} (MPa)	σ_{xm} (MPa)	σ_{ya} (MPa)	σ_{ym} (MPa)	δ (rad)	η_{exp} (rad)	η_{cal} (rad)
1	227.6	0.0	2.0	0.0	0	0	0
2	6.9	0.0	224.6	-2.9	π	$\pi/2$	$\pi/2$
3	233.5	52.0	191.3	41.2	0	0	0
4	171.7	-24.5	228.6	-11.8	0	$\pi/2$	$\pi/2$
5	121.6	11.8	156.0	-7.8	0	$\pi/2$	$\pi/2$
6	155.0	79.5	118.7	0.0	π	0	0

TABLE 2 - Comparison of experimental and calculated fatigue fracture plane position for Nishihara's tests (8).

	σ_{xa} (MPa)	σ_{xm} (MPa)	τ_{xya} (MPa)	τ_{xym} (MPa)	δ (rad)	η_{exp} (rad)	η_{cal} (rad)
1	0.0	0.0	201.1	0.0	0	0.25 π	0.25 π
2	141.9	0.0	171.3	0.0	0	0.19 π	0.19 π
3	142.0	0.0	171.2	0.0	$\pi/6$	0.18 π	0.19 π
4	255.1	0.0	127.5	0.0	0	0.12 π	0.13 π
5	255.1	0.0	127.5	0.0	$\pi/6$	0.09 π	0.12 π
6	308.0	0.0	63.9	0.0	0	0.06 π	0.06 π
7	323.7	0.0	0.0	0.0	0	0	0

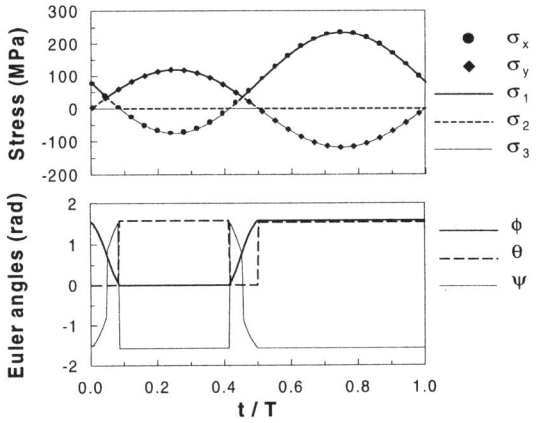

Fig. 4. Periodic time history of applied stresses, principal stresses and Euler angles for Rotvel's test No. 6 (Tab. 1).

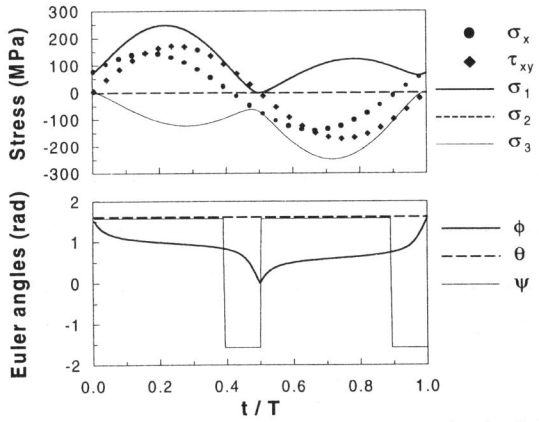

Fig. 5. Periodic time history of applied stresses, principal stresses and Euler angles for Nishihara's test No. 3 (Tab. 2).